



# Light emission by free electrons in photonic time-crystals

Alex Dikopoltsev<sup>a,1</sup>, Yonatan Sharabi<sup>a,1</sup>, Mark Lyubarov<sup>a</sup>, Yaakov Lumer<sup>a</sup>, Shai Tseses<sup>b</sup>, Eran Lustig<sup>a</sup>, Ido Kaminer<sup>b</sup>, and Mordechai Segev<sup>a,b,2</sup>

<sup>a</sup>Physics Department, Technion–Israel Institute of Technology, Haifa 32000, Israel; and <sup>b</sup>Electrical Engineering Department, Technion–Israel Institute of Technology, Haifa 32000, Israel

Contributed by Mordechai Segev; received October 30, 2021; accepted December 22, 2021; reviewed by Margaret Murnane and Eli Yablonovitch

**Photonic time-crystals (PTCs) are spatially homogeneous media whose electromagnetic susceptibility varies periodically in time, causing temporal reflections and refractions for any wave propagating within the medium. The time-reflected and time-refracted waves interfere, giving rise to Floquet modes with momentum bands separated by momentum gaps (rather than energy bands and energy gaps, as in photonic crystals). Here, we present a study on the emission of radiation by free electrons in PTCs. We show that a free electron moving in a PTC spontaneously emits radiation, and when associated with momentum-gap modes, the electron emission process is exponentially amplified by the modulation of the refractive index. Moreover, under strong electron–photon coupling, the quantum formulation reveals that the spontaneous emission into the PTC bandgap experiences destructive quantum interference with the emission of the electron into the PTC band modes, leading to suppression of the interdependent emission. Free-electron physics in PTCs offers a platform for studying a plethora of exciting phenomena, such as radiating dipoles moving at relativistic speeds and highly efficient quantum interactions with free electrons.**

photonics | ultrafast optics | photonic crystals | lasers

**P**hotonic time crystals (PTCs) are materials with a large time-periodic change of their electromagnetic properties. A sudden change in the optical properties leads to a time-reflection and time refraction for any electromagnetic wave traveling within that medium (1–4). Since causality dictates that time cannot be reversed, the reflected wave generated by the abrupt temporal variation (henceforth the time-reflected wave) cannot go back in time; instead, time-reflections go back in space, with a conjugate phase. Making a periodic sequence of changes in the material properties causes the forward-propagating (time-refracted) waves and the time-reflections to interfere, leading to the emergence of a band structure and dispersion relation (5–7). Naturally, PTCs seem similar to one-dimensional (1D) photonic crystals: The dispersion relations of the PTC and the photonic crystal are both determined by the strength and periodicity of the change in the electromagnetic properties. However, there are several profound fundamental differences between the two. First, while dielectric spatial photonic crystals conserve energy and do not conserve momentum, in PTCs, the temporal variations break time-translation symmetry, and therefore, energy is not a conserved quantity in PTCs. On the other hand, in spatially homogeneous media, PTCs conserve momentum. The conservation of momentum means that the  $k$ -wavevector is a good quantum number in the PTC (7). Second, the roles of  $\omega$  and  $k$  are swapped in the dispersion curve of a PTC, meaning that the bandgaps in the PTC are in momentum, rather than in energy (5, 7). The third difference has to do with the modes associated with the bandgap. A wave arriving at an air/dielectric photonic crystal interface with a frequency associated with the photonic crystal bandgap experiences total reflection because the photonic crystal has no propagating modes that can support such a frequency. In PTCs, on the other hand, because energy is

not conserved, waves with wavevectors inside the momentum gap change the energy they carry and exhibit not only exponential decay, but also exponential growth in time (8, 9).

To observe the main features of a PTC, such as the momentum gap (8), the modulation amplitude of the electromagnetic properties must be large (of order unity), and the modulation frequency should be high enough—on the order of the frequency of the electromagnetic wave propagating within the PTC. Otherwise, time-reflections become many orders of magnitude weaker than time-refracted light, which would lead to complete closure of the momentum bandgap, and the interaction becomes resonant, as in optical parametric amplifiers (OPAs) (10). Indeed, OPAs have been demonstrated to be a useful source of squeezed light (11, 12) under resonant conditions (the sum of the frequencies of the signal and idler equals the pump frequency and the phase-matching condition), but—in the absence of a bandgap—OPAs do not exhibit the unique properties of PTCs (*SI Appendix*). Given the extreme conditions required for the formation of a PTC, thus far, PTCs were demonstrated only at radio frequencies in electronic transmission lines (7). However, recent experimental advances in dynamic optical materials, especially in epsilon-near-zero (ENZ) materials (13, 14), hold the promise of having PTCs at optical frequencies very soon: Recent experiments showed large (on the order of  $\sim 1$ ), femtosecond-scale variations in the refractive index (15, 16). These and later experiments of time

## Significance

Recent experimental developments pave the way for the realization of photonic time-crystals (PTCs): photonic media with strong periodic variations of the optical properties occurring at single-cycle timescales. We study the radiation of free electrons in PTCs and show that the electron emission at half the modulation frequency is enhanced exponentially, drawing its energy from the modulation. When the electron is slower than the speed of light in the medium, the emitted light is fully controlled by the modulation. This radiation and its nonresonant nature hold promise for widely tunable laser sources, drawing their energy from the modulation, efficient laser-based particle accelerators, and particle detectors with adjustable angle-resolving sensitivity.

Author contributions: A.D., Y.S., M.L., Y.L., S.T., E.L., I.K., and M.S. designed research; A.D., Y.S., M.L., Y.L., E.L., and M.S. performed research; A.D., Y.S., M.L., Y.L., S.T., and M.S. analyzed data; and A.D., I.K., and M.S. wrote the paper.

Reviewers: M.M., University of Colorado Boulder; E.Y., University of California, Berkeley.

The authors declare no competing interest.

This article is distributed under [Creative Commons Attribution-NonCommercial-NoDerivatives License 4.0 \(CC BY-NC-ND\)](https://creativecommons.org/licenses/by-nc-nd/4.0/).

<sup>1</sup>A.D. and Y.S. contributed equally to this work.

<sup>2</sup>To whom correspondence may be addressed. Email: msegev@technion.ac.il.

This article contains supporting information online at <http://www.pnas.org/lookup/suppl/doi:10.1073/pnas.2119705119/-/DCSupplemental>.

Published February 7, 2022.

refraction (17–19) herald the possibility to experiment with PTCs in the near future (6, 20).

Here, we study the interaction of free electrons with PTCs. We show, through classical and quantum electrodynamic (QED) formulations, that free electrons propagating in a PTC spontaneously radiate due to the exchange of energy with their time-varying surrounding. The emission exhibits a tunable spectrum in two different regimes, subluminal and superluminal, displaying an abrupt transition in the shape of the radiation pattern when the electron becomes faster than the phase velocity of light in the medium and crosses the Cherenkov radiation threshold. The time-varying medium contributes an energy “kick” to the interaction, similar to Compton scattering, yet with the medium acting as the scattering photon. For electromagnetic waves with wavevectors  $k$  residing in the momentum gap, this energy kick leads to exponential amplification of the radiation, drawing the energy from the modulation. The QED analysis of the system with strong electron–photon coupling reveals an intriguing effect: The quantum degeneracy between the final states of the emission process by the moving electron and the states of the spontaneous emission created by vacuum fluctuations in the PTC is lifted by the interaction term and causes avoided crossing between the two processes. This causes the spontaneous emission into the momentum bandgap to display destructive quantum interference with the emission of the electron into PTC band modes, giving rise to suppression of the emission at the crossing point. The process of free-electron emission in PTCs, and especially the exponential enhancement of the emission driven by the temporally modulated refractive index, offer a plethora of new phenomena and suggest novel applications, such as widely tunable lasers ranging from the terahertz regime all the way to X-rays, drawing their energy from the modulation, and efficient laser-based particle accelerators.

Henceforth, we consider the radiation of an electron traveling in a PTC medium with  $\epsilon(t) = \epsilon(t + T)$ . The general geometry is presented in Fig. 1A, showing an electron moving at a constant velocity  $\beta c_0$  ( $c_0$  is the vacuum speed of light, and  $0 \leq \beta < 1$  is the velocity constant) inside a spatially homogeneous PTC while emitting radiation. In this geometry, it is notable to mention the work of Vitaly Ginzburg, who examined the radiation occurring under small (perturbative) modulation of the medium (21) and observed “transition scattering.” As stated earlier, here, we study the effects caused by the presence of the PTCs, which are highlighted by the existence of a momentum bandgap, within which radiation can be amplified exponentially. We assume a spatially infinite PTC, thereby excluding any edge effects associated

with dielectric interfaces. However, as we show in *SI Appendix*, a finite-bulk PTC produces the same features and interacts with the electron in a similar way, due to the miniscule size of the electron compared with the optical wavelength. Moreover, ultrafast ENZ materials and the recent progress in ultrafast transmission electron microscopes (UTEMs) (22) make the experimental platform for this phenomenon realizable (23). Fig. 1B presents a general outcome of a finite-difference time-domain (FDTD) simulation of Maxwell’s equations, displaying the electron radiation in a PTC of sinusoidal modulation  $\epsilon(t) = \epsilon_0 + \epsilon_1 \sin(\Omega t)$  starting at  $t = T_1$  and ending at  $t = T_2$  (the time analog of passing through a 1D photonic crystal of finite length). Importantly, this simulation is carried out for the case where the electron velocity is below the Cherenkov threshold; namely, the electron moves slower than the speed of light in the medium. Nevertheless, as Fig. 1B highlights, the temporal variations responsible for the PTC enable free-electron radiation, even in the regime that Cherenkov radiation cannot exist (24, 25). Moreover, since the PTC medium is homogeneous, all effects associated with a spatial periodicity [the Smith–Purcell effect (26)] do not exist either. Yet, the free electron displays efficient radiation, which is actually angle-dependent, despite the fact that the medium is homogeneous. Namely, as shown in Fig. 1B, waves at higher wavenumbers are emitted forward, closer to the propagation axis, while waves at lower wavenumbers are emitted backward. The results of this direct simulation immediately indicate that a free electron passing through a PTC radiates in a spatiotemporal pattern that is fundamentally different from known Cherenkov radiation.

To find the radiation of moving electrons in a PTC, we first analyze the electromagnetic modes in this time-modulated medium using Maxwell’s equations. Analogously to an abrupt change in space, a temporally abrupt change of the permittivity leads to time-reflection and time-refraction, both shifted in frequency (5). However, time-reflections cannot occur backward in time because (to the best of our knowledge) time only moves forward. Hence, time-reflections, even when generated by a spatially uniform temporal change in the medium, actually occur in space and appear as spatial back-reflections. Naturally, when the susceptibility in a medium undergoes periodic changes in time, the refractive index variations induce multiple reflections and refractions of waves in space. Due to the periodicity of the variations, the reflections and refractions interfere to form a Floquet band structure of the electromagnetic modes (Fig. 24). When the medium is homogeneous, the wavevector  $\mathbf{k}$  is a conserved quantity appearing as a constant characterizing each eigenmode.

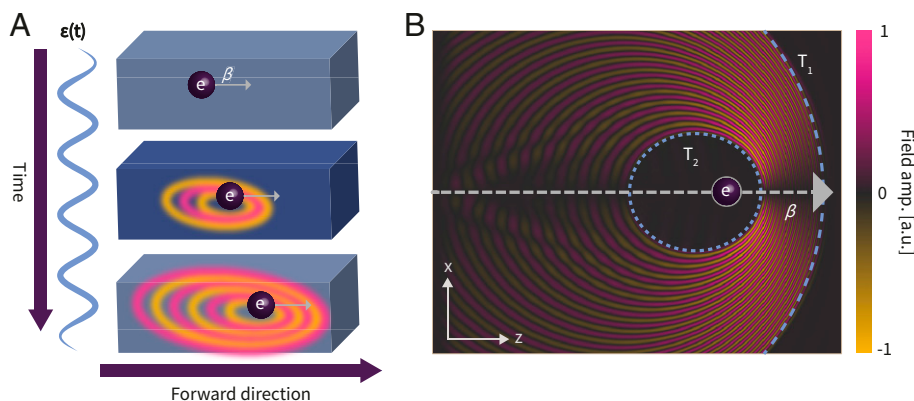


**Fig. 1.** The process of free-electron radiation in a PTC. (A) Schematics of a free electron moving and radiating in a PTC. When the index of refraction changes periodically in time, the electron moving in the medium emits electromagnetic radiation, which depends on the modulation and on the electron velocity  $\beta c_0$ . (B) Magnetic field amplitude (amp.) of the electromagnetic radiation,  $H(x, y = 0, z, t)$ , obtained by FDTD simulation for an electron moving at velocity  $\beta c_0$  in a PTC of 20 cycles that starts at time  $t = T_1$  and ends at  $t = T_2$ ; the snapshot is taken at  $t > T_2$ . High wavenumbers are emitted backward. There is no radiation on the propagation axis because the polarization of the emitted waves cannot be perpendicular to the electron velocity. a.u., arbitrary units.

The Floquet modes of the electromagnetic field are conveniently expressed through the magnetic field (because its mathematical relation to the current source is free of time-derivatives) of the form  $\mathbf{H}_{\mathbf{k}}(\mathbf{r}, t) = \mathbf{H}_0 e^{i\mathbf{k}\cdot\mathbf{r}} h_{\mathbf{k}}(t)$ ;  $h_{\mathbf{k}}(t) = e^{i\omega_{\mathbf{k}} t} \sum q_{\mathbf{k}}^m e^{im\Omega t}$ , where  $\omega_{\mathbf{k}}$  is the Floquet frequency that depends on the wavenumber  $\mathbf{k}$ ,  $\Omega$  is the modulation frequency  $2\pi/T$  ( $T$  is the period),  $m$  is the order of the harmonic, and  $q_{\mathbf{k}}^m$  are the coefficients of the Floquet mode harmonic. Notice that, for each wavenumber  $\mathbf{k}$ , there are two Floquet function solutions,  $h_{\mathbf{k},+}(t)$  and  $h_{\mathbf{k},-}(t)$ , for  $\omega_{\mathbf{k}}$  and  $-\omega_{\mathbf{k}}$ , respectively. When  $\mathbf{k}$  is in the band, these functions are complex conjugates,  $h_{\mathbf{k},+}(t) = h_{\mathbf{k},-}^*(t)$ . But when  $\mathbf{k}$  is in the gap,  $\omega_{\mathbf{k}}$  becomes complex; therefore, one of the solutions is decaying exponentially, and one is growing exponentially with time (*SI Appendix*). For these momentum-gap modes, the energy carried by the modes grows or decays exponentially, at the expense of the energy invested in the temporal modulation of the permittivity. The superposition of all modes in the bands and in the gaps, each with its own wavenumber  $\mathbf{k}$ , describes the electromagnetic surrounding of the electron passing through the PTC.

We model the electron classically, as a point charge moving in the  $z$  direction, with velocity  $v = \beta c_0$ , creating electric current density  $\mathbf{j}_e(\mathbf{r}, t) = \delta(r_{\perp}) \delta(z - \beta c_0 t) \hat{z}$ , where  $r_{\perp}$  are the coordinates transverse to  $z$ . The point source can be decomposed into its spatial wavenumbers  $\mathbf{j}_{\mathbf{k}}(\mathbf{r}, t) = j_0 e^{i\mathbf{k}\cdot\mathbf{r}} \delta(z - \beta c_0 t) \hat{z}$ . The wave equation for the magnetic field component  $\mathbf{H}_{\mathbf{k}}$  in a PTC with a current source  $\mathbf{j}_{\mathbf{k}}$  is

$$\left( \partial_t (\varepsilon_m(t) \partial_t) - c^2 k^2 \right) \mathbf{H}_{\mathbf{k}}(t) = -i\mathbf{k} \times \mathbf{j}_{\mathbf{k}}, \quad [1]$$

where  $c = 1/\sqrt{\mu_0 \varepsilon_0 \varepsilon_m(t)}$ , and the permittivity is  $\varepsilon(t) = \varepsilon_0 \varepsilon_r(t) \varepsilon_m(t)$ , where  $\varepsilon_m(t)$  is the time-dependent part and  $\varepsilon_m(0) = 1$ . To solve this equation, we find the Green function, which satisfies the time-dependent part of Eq. 1,  $(\partial_t (\varepsilon_m(t) \partial_t) - c^2 k^2) G_{\mathbf{k}}(t, t') = \delta(t - t')$ . Using the time-dependent part of the magnetic field,  $h_{\mathbf{k}}(t)$ , we find (details in *SI Appendix*)

$$G_{\mathbf{k}}(t, t') = \begin{cases} \frac{h_{\mathbf{k},+}(t') h_{\mathbf{k},-}(t) - h_{\mathbf{k},-}(t') h_{\mathbf{k},+}(t)}{C_{\mathbf{k}}} & t < t' \\ 0 & t \geq t' \end{cases}, \quad [2]$$

where  $C_{\mathbf{k}} = \varepsilon(t) (h_{\mathbf{k},+}(t) h_{\mathbf{k},-}(t) - h_{\mathbf{k},-}(t) h_{\mathbf{k},+}(t))$  is constant in time, which, interestingly, is proportional to the Minkowski momentum,  $\int (\mathbf{D} \times \mathbf{B}) dV$  (27). The Minkowski momentum is a conserved quantity for a homogenous medium, even when the medium varies in time, and is used here to define the amplitude of each mode. By integrating over the product of the Green function and our current source,  $\mathbf{j}_{\mathbf{k}}$ , we find the electromagnetic radiation induced by the electron. The radiation efficiency of the electron is determined by the relation between its phase  $k_z \beta c_0 t$  and the phase of the Floquet modes  $h_{\mathbf{k}}(t)$ , a necessary requirement for efficient light emission of free electrons in matter. Maximum efficiency occurs when the phases match—that is, when  $k_z \beta c_0 = \omega_{\mathbf{k}} + m\Omega$ —which occurs for every wavenumber  $\mathbf{k}$  and harmonic number  $m$  separately. These considerations allow for phase matching of the radiation process in time and the  $z$  direction simultaneously, which results in the following magnetic field component:

$$H_{k_x/y, m}(t) = -i \frac{k_x/y h_{\mathbf{k}}(t) q_{\mathbf{k}}^{m*} t}{2C_{\mathbf{k}}}. \quad [3]$$

We find that the amplitude of the field grows with time and is proportional to the strength of the relevant Floquet harmonic,  $|q_{\mathbf{k}}^m|$ . Moreover, when the wavenumber of the source resides in the momentum gap, any coupling to that gap mode induces exponential growth of the radiation amplitude, in line with the exponential growth of  $h_{\mathbf{k},+}(t)$  (see the analytical derivation in *SI Appendix*).

To find the exact angles and frequencies to which the electron radiates, we map the phase-matching condition onto the wavevector space  $(k_z, k_{\perp})$  of radiation in the PTC

$$k_{\perp}^2 = k_z^2 (n_{\text{eff}}^2(k) \beta^2 - 1) - 2mk_z \beta n_{\text{eff}} k_{\text{mod}} + m^2 k_{\text{mod}}^2, \quad [4]$$

where  $n_{\text{eff}}(k) = \omega_{\mathbf{k}}/k c_0$  and  $k_{\text{mod}} = \Omega n_{\text{eff}}/c_0$ . This mapping is natural because the wavevector  $\mathbf{k}$  is a conserved quantity for each mode in our system. Fig. 2B and C show this mapping in two distinct cases, where the electron is below and above the Cherenkov velocity threshold, respectively. The Cherenkov threshold ( $\beta n_r = 1$ ) plays a significant role in this interaction—it differentiates between two regimes of radiation, subluminal and superluminal. We notice that the main harmonic ( $k_z \beta c_0 = \omega_{\mathbf{k}}$ ;  $m = 0$ ) is missing in the subluminal regime, where  $\beta = 0.4 < 1/n_r$  (Fig. 2B). This is because the electron is not fast enough on its own to radiate, for the very same reason that there is no Cherenkov radiation below the threshold. However, because the medium here is a PTC, the temporal modulation of the permittivity endows the electron with energy to interact with frequencies of integer quanta  $\Omega$  higher and lower than the Floquet frequency  $\omega_{\mathbf{k}}$  of the radiated modes. For example, when phase matching is met for harmonic  $m = -1$ , with  $k_z \beta c_0 = \omega_{\mathbf{k}} - \Omega$ , radiation is efficiently emitted into this Floquet mode with its original frequency  $\omega_{\mathbf{k}}$ . On the other hand, in the superluminal regime (Fig. 2C) with  $\beta = 0.99 > 1/n_r$ , the electron is fast enough not only to emit ordinary Cherenkov radiation, which is here modified by the PTC dispersion ( $m = 0$ ), but also to radiate to higher harmonics with  $m > 0$ . Moreover, in the superluminal regime, the phase-matching condition is fulfilled also for gap modes. The coupling varies according to the shape of the bandgap modes (*SI Appendix*), but after being excited by the electron—all gap radiation grows exponentially.

To confirm our analytical results, we simulate this system with an FDTD algorithm. Fig. 2D shows a comparison between the magnetic field amplitude found in simulations and the analytic calculation, for an electron moving with  $\beta = 0.4$  in a medium with permittivity  $\varepsilon(t) = 2 + 0.2 \sin(\Omega t)$ , at the end of 50 PTC cycles. The simulation results conform well for the full range of angles (up to the resolution and system size limits of FDTD simulations). Fig. 2E and F display the Fourier components of the output magnetic field for  $\beta = 0.4$  and 0.99, respectively (same as in Fig. 2B and C), when  $\varepsilon_1/\varepsilon_0 = 0.2$ . These simulations show that the electron radiation indeed follows the phase-matching condition presented above for the Floquet band modes. But even more interestingly, when the electron radiates into phase-matched modes within the bandgap, the radiation grows exponentially in time (analytic expression given in *SI Appendix*).

Thus far, we treated the free electron as a classical moving point charge and showed that the emitted electromagnetic radiation strongly depends on the band structure of the PTC. In the subluminal (spectrally limited) case ( $\beta n < 1$ ), the PTC serves as an “enabler” for the electron radiation, where the free electron is phase-matched to harmonics with  $m < 0$ . In the superluminal regime ( $\beta n > 1$ ), the free electron is phase-matched with all the harmonics of the PTC modes, so in addition to the fundamental harmonic ( $m = 0$ ), which corresponds partially to the ordinary Cherenkov radiation in a stationary medium, we find superluminal radiation in a slew of frequencies and angles. The classical model we use predicts these outcomes, yet, it is incomplete in explaining the free-electron emission to momentum-gap modes. This is because—as we show below—a medium that is modulated in time also displays spontaneous photon-pair creation exactly in the momentum gap, and this emission grows exponentially and interferes with the PTC Cherenkov-like radiation. Naturally, this phenomenon cannot be explained through Maxwell’s equations. Next, we present the quantum model to complete

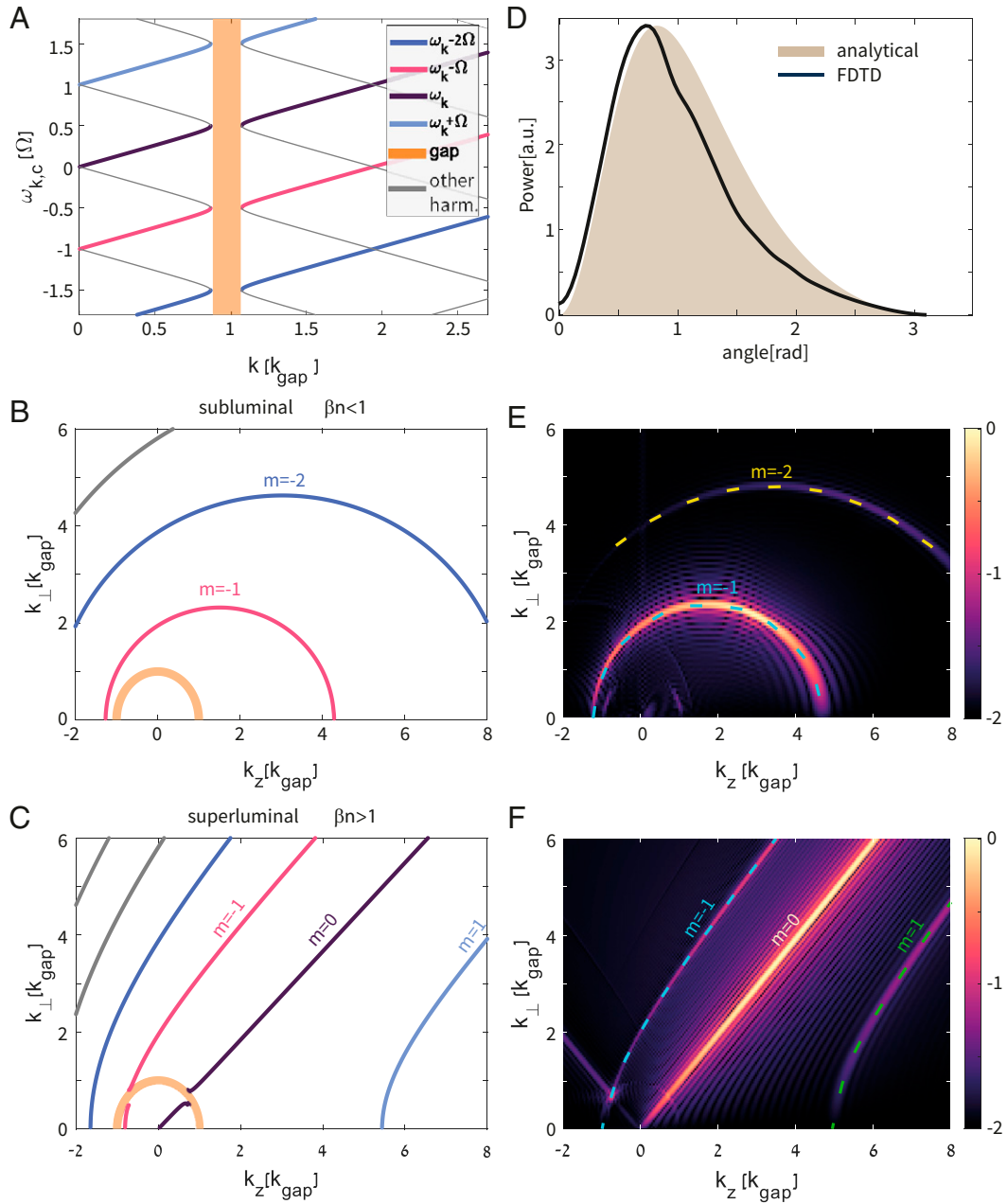


**Fig. 2.** Band structure of the PTC and the radiation emitted by the free electron. (A) Unfolded band structure of the PTC, with the momentum gap marked in orange and the various bands marked in different colors. Here,  $k_{\text{gap}} = \Omega n_r / 2c_0$ , where  $\Omega$  is the PTC modulation frequency and  $n_r = \sqrt{\epsilon_r}$  is the bias refractive index, and the modulation strength is  $\epsilon_1/\epsilon_0 = 0.4$ . The units of the floquet frequency,  $\omega_{k,c}$ , and the wavenumbers are normalized to  $\Omega$  and  $k_{\text{gap}}$ , respectively. The changes of the permittivity in time cause reflections and refractions that lead to the buildup of the Floquet band structure. (B and C) Phase-matched lines marking the directions of efficient radiation emitted by a free electron moving through a PTC, in the subluminal and in the superluminal regimes, respectively. (D) Power carried by the electromagnetic radiation vs. radiation angle for  $\beta = 0.4$ : comparison between the analytic result and the FDTD simulation. (E and F) Radiation pattern calculated by FDTD simulations in the subluminal and superluminal regimes, respectively. The radiation lines correspond to the lines in B and C. harm., harmonics.

the physical picture of light emission by a free electron moving in a PTC.

To describe the underlying phenomena on a single-photon interaction level, we use canonical quantization tools. The resulting Hamiltonian of our system is (see details in *SI Appendix*):

$$\begin{aligned}
 H_{\text{tot}} &= H_{EM}(t) + H_e + H_I \\
 &= \sum_{k,\sigma} \hbar \frac{c_0 |k|}{n_r} \left( \left( \frac{\epsilon_m(t) + 1}{2\epsilon_m(t)} \right) \left( a_{k\sigma}^\dagger a_{k\sigma} + \frac{1}{2} \right) + \left( \frac{\epsilon_m(t) - 1}{4\epsilon_m(t)} \right) \right. \\
 &\quad \left. \times (a_{k\sigma} a_{-k\sigma} + a_{k\sigma}^\dagger a_{-k\sigma}^\dagger) \right) + \frac{\hat{\mathbf{P}}^2}{2m} - \frac{e\hat{\mathbf{P}} \cdot \hat{\mathbf{A}}}{m}
 \end{aligned} \quad [5]$$

with  $n_r = \sqrt{\epsilon_r}$ . This expression consists of the Hamiltonians for the electromagnetic field  $H_{EM}$ , the free-electron energy  $H_e$ , and the interaction term  $H_I$ , where  $n_r$  is the ambient refractive index,  $\mathbf{k}$  and  $\sigma$  are the wavenumber and polarization,  $\epsilon(t)$  is the modulated permittivity,  $a_{k,\sigma}^\dagger, a_{k,\sigma}$  are the creation and annihilation operators of a photon with  $k$  and  $\sigma$ ,  $\hat{\mathbf{P}}$  is the momentum operator of the electron, and  $\hat{\mathbf{A}}$  is the vector potential operator of the electromagnetic field, written using  $a_{k\sigma}$  (*SI Appendix*). Notice that  $H_{EM}(t)$  contains terms describing the creation and annihilation of pairs of photons with opposite momenta  $\hbar\mathbf{k}$  and  $-\hbar\mathbf{k}$ , highlighting the fact that the total momentum is

conserved. We can therefore arrange the states in independent ladders of pairs of counterpropagating photons with wavevectors  $\mathbf{k}$  and  $-\mathbf{k}$ ,  $|0_k, 0_{-k}\rangle$ ,  $|1_k, 1_{-k}\rangle$ ,  $|2_k, 2_{-k}\rangle$ , etc. The last term of  $H_{EM}$  couples these states by adding (or subtracting) precisely one pair of  $k$  and  $-k$  photons, thus not changing the overall momentum. For wavevectors residing in the gap, the number of photons increases exponentially, even if initially, there were no such photons in the medium; i.e., these photons can appear spontaneously from vacuum fluctuations (28–31)—a pure QED effect. It is essential here to highlight the importance of the momentum gap: In a PTC, these photon pairs appear at any frequency, as long as their wavenumber is associated with the gap, unlike the generation of squeezed light in OPAs (11), which appears under strict resonant conditions (see discussion in *SI Appendix* comparing PTCs and OPAs).

To study the free-electron interaction with photons in such a medium, we add the terms of the electron energy  $H_e$  and the interaction term  $H_I$ . As in the classical model, here, too, we find the same type of radiation, in addition to the ordinary Cherenkov radiation. This radiation is caused by the exchange of energy quanta  $\hbar\Omega$  between the electron and the PTC. The relation between the wavevector of the emitted photon and the electron velocity is simply given by energy and momentum conservation of the interaction process (*SI Appendix*), which results in  $k_z\beta c_0 = \omega - \ell\Omega$ . This relation seems exactly equivalent to the classical relation we derived earlier; however—from a QED perspective— $\ell$  is the number of energy quanta  $\hbar\Omega$  delivered from the PTC to the emitted photon in the interaction process. Fig. 3A shows the probability of the electron to emit a photon in a PTC in the subluminal regime, in a region of wavevectors located far from the momentum gap. This radiation conforms at most wavevectors with the radiation we found using the classical analysis, based on Maxwell's equations (pink line). The emission probability is especially high when the energy-conservation condition for the  $\ell = 1$  harmonic is fulfilled, i.e.,  $k_z\beta c_0 = \omega - \Omega$ . In this case, the electron contributes a quantum of energy  $\hbar(\omega - \Omega)$  and emits a photon with energy  $\hbar\omega$ , which means that the PTC (the modulation of the refractive index) contributed energy of  $\hbar\Omega$  to this interaction. The superluminal regime is even more interesting. When the velocity of the electron crosses the speed of light in the medium, an abrupt transition occurs in the radiation pattern: We find both the ordinary Cherenkov-type (shockwave) radiation at angle  $\theta_{Ch} = \cos^{-1}(1/\beta n_{eff}(k))$  ( $\ell = 0$ ) when the PTC does not contribute energy to the process and an important additional outcome: the electron-PTC interaction for  $\ell < 0$ . In this latter case, the electron contributes the energy quanta  $\hbar(\omega + |\ell|\Omega)$ , but the energy of each emitted photon is still  $\hbar\omega$ . This means that when the electron emits radiation to these modes, it also returns energy back to the modulated medium. In this process, the electron slows down more than it does when it emits ordinary Cherenkov

radiation in a stationary medium with the relation  $\Delta\beta = \frac{(1-\beta_i^2)^{\frac{3}{2}}}{\beta_i m_0 c_0^2}$   $\hbar(\omega + \ell\Omega)$ , where  $\beta_i$  is the initial velocity of the electron and  $\Delta\beta$  is the change in the electron velocity due to the emission of a photon with energy  $\hbar\omega$  and the loss of energy  $\hbar\ell\Omega$  to the PTC (see *SI Appendix* for more details).

Another intriguing emission regime occurs in the momentum-gap region. In the momentum gap, pairs of photons with opposite momentum are spontaneously emitted out of vacuum, similar to the dynamic Casimir effect, where moving boundaries of a cavity create pairs of photons with half the modulation frequency (32). Using Eq. 5 to study the quantum interaction of an electron and momentum-gap photons of the PTC, we find (Fig. 3B) that the photon emission rate increases exponentially (deep purple) compared to the emission rate without the PTC (pink).

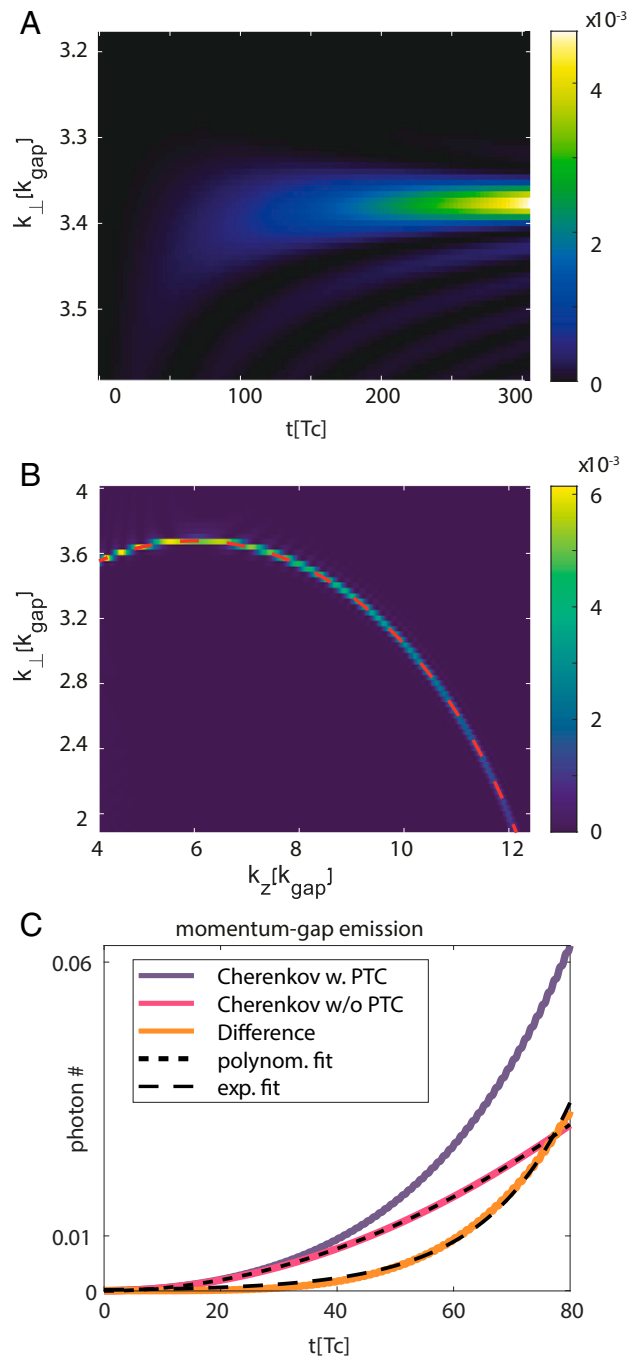


**Fig. 3.** Free-electron interaction with single photons in a PTC. (A) Photon emission probability as a function of time in a range of  $k$ -wavenumbers, emitted by a free electron moving in a PTC with  $\beta = 0.6$ ,  $\epsilon_1/\epsilon_0 = 0.1$ , and  $g/\omega = 7.8 \times 10^{-3}$ . The units of time are normalized to the modulation cycle time,  $T_c = 2\pi/\Omega$ . (B) Photon emission probability by a free electron ( $\beta = 0.6$ ) moving in a PTC, as a function of the  $k$ -vector of the emitted photon, as observed after 300 PTC cycles. The dashed red line marks the angles of phase-matching between the electron and the electromagnetic waves (via the classical model), corresponding well to the calculated probability of emission. Both A and B are calculated with the Hamiltonian of Eq. 5. (C) Cherenkov radiation of an electron with  $\beta = 0.9$  in a PTC (deep purple) compared to ordinary Cherenkov without a PTC (pink) as a function of time for wavenumbers residing in the momentum-gap center of the PTC, with  $\epsilon_r(t) = 2 + 0.05\sin(\omega t)$  and coupling strength  $g/\omega = 10^{-5}$ . The difference between emission with (w.) and without (w/o) the PTC (orange) follows an exponential (exp.) fit (long-dashed black line). The number of photons emitted by the electron is exponentially enhanced, drawing energy from the temporal modulation of the refractive index. polynom., polynomial.

exponential growth is shown by fitting the difference in emission rates to an exponential function (orange). This finding stands in sharp contrast to suppressed (prohibited) emission of photons in the bandgap of spatial photonic crystals (33). We believe this is a general feature of emission into a time-varying medium: The emission rate is always higher for photons with wavenumbers  $k$  inside a PTC momentum gap.

In the same superluminal regime and under strong electron-photon coupling, characterized by the coupling strength  $g$ , we find an even more interesting effect at the angle opposite to the ordinary Cherenkov angle. In that direction, the final states of the emission process by the moving electron,  $|P - \hbar k, n_k, n_{-k} - 1\rangle$ , become quantum-degenerate with the states of the spontaneous emission created by vacuum fluctuations and enhanced by the PTC,  $|P, n_k, n_{-k}\rangle$ . This quantum degeneracy of momentum and energy is lifted by the interaction term and causes avoided crossing between the two processes, as shown by Fig. 4A. We mark the lines of electron radiation in a PTC with very weak electron-photon coupling (pink) and the bandgap wavevectors (orange). In principle, these lines would cross, but the strong interaction between the electron and the medium prevents the crossing. Fig. 4B shows the growing emission probability at two new wavevectors,  $k_{\text{gap}} \pm \Delta k$ , where  $\Delta k$  depends on the electron-photon interaction strength. Fig. 4C compares the spontaneous two-photon emission over time, in the absence and in the presence of a free electron. When the electron is absent, the photon pairs are created in a rate that grows exponentially.

The presence of the free electron alters the process dramatically: The emission in the PTC momentum gap is suppressed at the crossing point, highlighting the avoided crossing. Fig. 4D, on the other hand, compares the radiation at the two wavevectors, with  $k_{\perp} = k_{\text{gap}} \pm \Delta k$ . It shows that emission at these wavevectors is enhanced due to the presence of the electron. These results are direct outcome of the underlying QED mechanism, as they cannot be explained through the Maxwell equations alone.

In conclusion, we analyzed the emission of radiation by a free electron moving through a PTC, predicted the exponential enhancement of emission in the directions conforming to the momentum gap, and pinpointed the outcome of QED in the form of avoided crossing. Our classical and quantum descriptions of the electromagnetic modes and electron interaction are general and can be applied to any variation of the permittivity in time, strong and abrupt as it may be. The recent progress on ultrafast ENZ materials makes it promising to observe PTCs in the near future, and the utilization of UTEMs (22) makes the ideas described here accessible to experiments (23) (see detailed suggestions for an experiment in *SI Appendix*). Specifically, the recently developed ENZ materials with strong non-linear effects were shown to possess very fast (femtosecond) and strong (order of  $\sim 1$ ) modulation of the permittivity in response to an ultrafast pulse, already showing time refraction (15, 18, 34) and features of time-reflection (19). In principle, a train of such pulses will result in time-periodic permittivity—creating a PTC, and then a free electron in this PTC will effectively acts as a

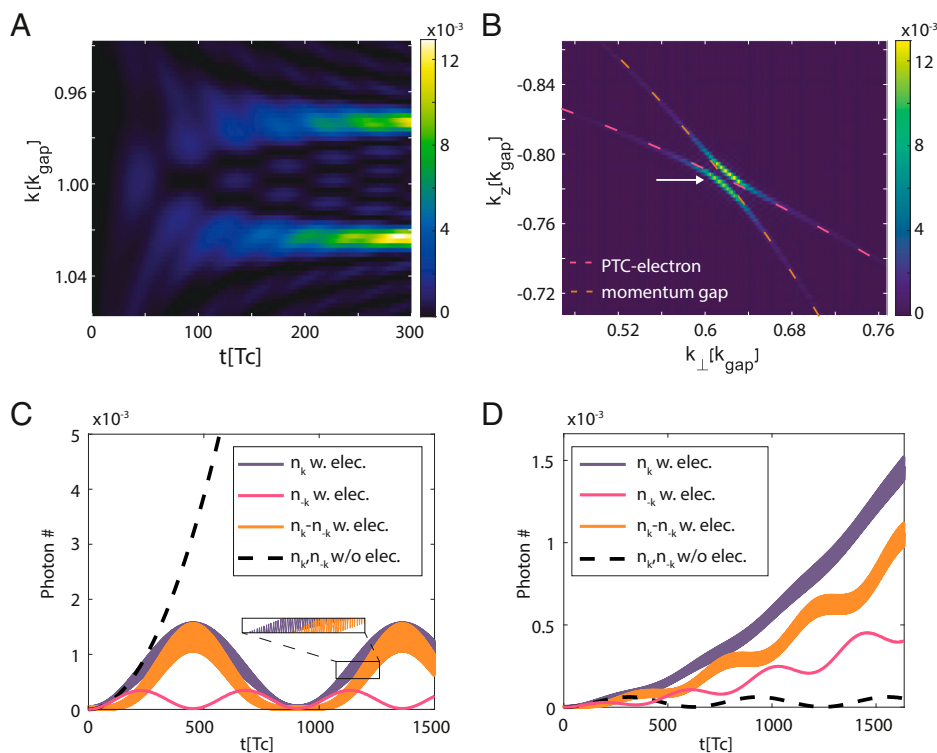


**Fig. 4.** Free-electron back-emission near the momentum gap of a PTC ( $\beta = 0.9$ ). (A) Probability of the electron to emit a photon after 300 Tc. The electromagnetic radiation at the gap enhances the probability for the electron to emit a photon, which reaches a maximum at the momentum gap (dashed pink), but this point coincides with the probability for spontaneously emitted photon pairs (dashed orange). The quantum interference between these two distinct effects results in avoided crossing. The size of the splitting depends on the light-matter interaction strength; here,  $g\omega = 2.2 \times 10^{-2}$ . (B) Probability of photon emission in the back-direction of the electron near the momentum gap vs. time ( $k$ -wavevectors that belong to the dashed black line from A). The splitting becomes evident after several tens of modulation cycles in the permittivity. The electron-photon coupling strength is  $g\omega = 7.8 \times 10^{-3}$ . (C) Comparison of the back-emission in the PTC momentum gap with (w.) and without (w/o) the electron (elec.). The presence of the electron suppresses the spontaneous two-photon emission in the gap. (D) Comparison of the back-emission in the band, but near a PTC momentum gap, at  $k$ -wavevector in the region of avoided crossing, with and without the electron: Here, the presence of the electron enhances the radiation emission. The coupling strength for C and D is  $g\omega = 3 \times 10^{-3}$ . We chose weak modulation amplitudes  $\varepsilon_1/\varepsilon_0 = 2 \times 10^{-3}$  for A and B and  $10^{-4}$  for C and D to stay in the perturbative limits of the quantum simulations. The Inset in C highlights the modulation within each cycle.

relativistic electromagnetic emission source. This scheme can pave the way to new physics, such as a radiation scheme for relativistic dipoles known to show effects like the superlight inverse Doppler effect (35) or the study of quantum correlations between electrons and the photon pairs created by the modulation (36). Looking forward, these ideas could also lead to novel tunable particle detectors (37) and particle accelerators (38, 39) and to free-electron X-ray lasers (40–43) drawing their

energy from periodically driven materials, which can be tuned over a large wavelength span.

**Data Availability.** All study data are included in the article and/or *SI Appendix*.

**ACKNOWLEDGMENTS.** This work was partially funded by the US Air Force Office of Scientific Research, which supported our research on topological photonics, through which we came up with the ideas of PTCs.

1. F. R. Morgenthaler, Velocity modulation of electromagnetic waves. *IEEE Trans. Microw. Theory Tech.* **6**, 167–172 (1958).
2. D. E. Holberg, K. S. Kunz, Parametric properties of fields in a slab of time-varying permittivity. *IEEE Trans. Antenn. Propag.* **14**, 183–194 (1966).
3. J. T. Mendonça, P. K. Shukla, Time refraction and time reflection: Two basic concepts. *Phys. Scr.* **65**, 160 (2002).
4. V. Bacot, M. Labousse, A. Eddi, M. Fink, E. Fort, Time reversal and holography with spacetime transformations. *Nat. Phys.* **12**, 972–977 (2016).
5. F. Biancalana, A. Amann, A. V. Uskov, E. P. O'Reilly, Dynamics of light propagation in spatiotemporal dielectric structures. *Phys. Rev. E Stat. Nonlin. Soft Matter Phys.* **75**, 046607 (2007).
6. J. R. Zurita-Sánchez, P. Halevi, J. C. Cervantes-González, Reflection and transmission of a wave incident on a slab with a time-periodic dielectric function. *Phys. Rev. A* **79**, 053821 (2009).
7. J. R. Reyes-Ayona, P. Halevi, Observation of genuine wave vector ( $k$  or  $\beta$ ) gap in a dynamic transmission line and temporal photonic crystals. *Appl. Phys. Lett.* **107**, 074101 (2015).
8. E. Lustig, Y. Sharabi, M. Segev, Topological aspects of photonic time crystals. *Optica* **5**, 1390 (2018).
9. Y. Sharabi, E. Lustig, M. Segev, Disordered photonic time crystals. *Phys. Rev. Lett.* **126**, 163902 (2021).
10. J. A. Giordmaine, Mixing of light beams in crystals. *Phys. Rev. Lett.* **8**, 19–20 (1962).
11. R. E. Slusher, L. W. Hollberg, B. Yurke, J. C. Mertz, J. F. Valley, Observation of squeezed states generated by four-wave mixing in an optical cavity. *Phys. Rev. Lett.* **55**, 2409–2412 (1985).
12. B. Yurke *et al.*, Observation of 4.2-K equilibrium-noise squeezing via a Josephson-parametric amplifier. *Phys. Rev. Lett.* **60**, 764–767 (1988).
13. M. Silveirinha, N. Engheta, Tunneling of electromagnetic energy through subwavelength channels and bends using epsilon-near-zero materials. *Phys. Rev. Lett.* **97**, 157403 (2006).
14. A. Alù, M. G. Silveirinha, A. Salandrino, N. Engheta, Epsilon-near-zero metamaterials and electromagnetic sources: Tailoring the radiation phase pattern. *Phys. Rev. B Condens. Matter Mater. Phys.* **75**, 155410 (2007).
15. L. Caspani *et al.*, Enhanced nonlinear refractive index in  $\epsilon$ -near-zero materials. *Phys. Rev. Lett.* **116**, 233901 (2016).
16. M. Z. Alam, I. De Leon, R. W. Boyd, Large optical nonlinearity of indium tin oxide in its epsilon-near-zero region. *Science* **352**, 795–797 (2016).
17. Y. Zhou *et al.*, Broadband frequency translation through time refraction in an epsilon-near-zero material. *Nat. Commun.* **11**, 2180 (2020).
18. V. Bruno *et al.*, Negative refraction in time-varying strongly coupled plasmonic-antenna-epsilon-near-zero systems. *Phys. Rev. Lett.* **124**, 043902 (2020).
19. E. Lustig *et al.*, "Towards photonic time-crystals: Observation of a femtosecond time-boundary in the refractive index," in *2021 Conference on Lasers and Electro-Optics (CLEO)* (IEEE, Piscataway, NJ, 2021), pp. 1–2.
20. J. R. Zurita-Sánchez, J. H. Abundis-Patiño, P. Halevi, Pulse propagation through a slab with time-periodic dielectric function  $\epsilon(t)$ . *Opt. Express* **20**, 5586–5600 (2012).
21. V. L. Ginzburg, Transition radiation and transition scattering. *Phys. Scr.* **T2A**, 182–191 (1982).
22. B. Barwick, D. J. Flannigan, A. H. Zewail, Photon-induced near-field electron microscopy. *Nature* **462**, 902–906 (2009).
23. R. Dahan *et al.*, Resonant phase-matching between a light wave and a free-electron wavefunction. *Nat. Phys.* **16**, 1123–1131 (2020).
24. P. A. Cherenkov, Visible emission of clean liquids by action of gamma radiation. *Dokl. Akad. Nauk SSSR* **2**, 451–454 (1934).
25. I. E. Tamm, I. M. Frank, Coherent radiation of fast electrons in a medium. *Dokl. Akad. Nauk SSSR* **14**, 109–114 (1937).
26. S. J. Smith, E. M. Purcell, Visible light from localized surface charges moving across a grating. *Phys. Rev.* **92**, 1069 (1953).
27. S. M. Barnett, R. Loudon, The enigma of optical momentum in a medium. *Philos. Trans. R. Soc. A Math. Phys. Eng. Sci.* **368**, 927–939 (2010).
28. L. Parker, Quantized fields and particle creation in expanding universes. I. *Phys. Rev.* **183**, 1057–1068 (1969).
29. C. K. Law, Effective Hamiltonian for the radiation in a cavity with a moving mirror and a time-varying dielectric medium. *Phys. Rev. A* **49**, 433–437 (1994).
30. T. Kawakubo, K. Yamamoto, Photon creation in a resonant cavity with a nonstationary plasma mirror and its detection with Rydberg atoms. *Phys. Rev. A* **83**, 13819 (2011).
31. E. Yablonovitch, Accelerating reference frame for electromagnetic waves in a rapidly growing plasma: Unruh-Davies-Fulling-DeWitt radiation and the nonadiabatic Casimir effect. *Phys. Rev. Lett.* **62**, 1742–1745 (1989).
32. G. T. Moore, Quantum theory of the electromagnetic field in a variable-length one-dimensional cavity. *J. Math. Phys.* **11**, 2679–2691 (1970).
33. E. Yablonovitch, Inhibited spontaneous emission in solid-state physics and electronics. *Phys. Rev. Lett.* **58**, 2059–2062 (1987).
34. A. Shaltout, A. Kildishev, V. Shalaev, Time-varying metasurfaces and Lorentz nonreciprocity. *Opt. Mater. Express* **5**, 2459–2467 (2015).
35. X. Shi *et al.*, Superlight inverse Doppler effect. *Nat. Phys.* **14**, 1001–1005 (2018).
36. R. Dahan *et al.*, Imprinting the quantum statistics of photons on free electrons. *Science* **373**, eabj7128 (2021).
37. T. Ypsilantis, J. Seguinot, Theory of ring imaging Cherenkov counters. *Nucl. Instruments Methods Phys. Res. Sect. A Accel. Spectrometers. Detect. Assoc. Equip.* **343**, 30–51 (1994).
38. C. M. S. Sears *et al.*, High-harmonic inverse-free-electron-laser interaction at 800 nm. *Phys. Rev. Lett.* **95**, 194801 (2005).
39. Y. Adiv *et al.*, Quantum nature of dielectric laser accelerators. *Phys. Rev. X* **11**, 41042 (2021).
40. G. Adamo *et al.*, Light well: A tunable free-electron light source on a chip. *Phys. Rev. Lett.* **103**, 113901 (2009).
41. A. M. Cook *et al.*, Observation of narrow-band terahertz coherent Cherenkov radiation from a cylindrical dielectric-lined waveguide. *Phys. Rev. Lett.* **103**, 095003 (2009).
42. F. Liu *et al.*, Integrated Cherenkov radiation emitter eliminating the electron velocity threshold. *Nat. Photonics* **11**, 289–292 (2017).
43. L. J. Wong, I. Kaminer, O. Ilic, J. D. Joannopoulos, M. Soljačić, Towards graphene plasmon-based free-electron infrared to X-ray sources. *Nat. Photonics* **10**, 46–52 (2016).